IEEE Access
Multidisciplinary | Rapid Review | Open Access Journal

Received April 17, 2019, accepted June 26, 2019, date of publication July 10, 2019, date of current version July 26, 2019.

Digital Object Identifier 10.1109/ACCESS.2019.2927793

Internet of Things Based Monitoring of Large Rotor Vibration With a Microelectromechanical Systems Accelerometer

IVAR KOENE, RAINE VIITALA, AND PETRI KUOSMANEN
Department of Mechanical Engineering, Aalto University, 02150 Espoo, Finland

Corresponding author: Ivar Koene (ivar.koene@aalto.fi)

This work was supported by the Academy of Finland, Digital Twin of Rotor System, under Grant 313675.

ABSTRACT In rotating machinery, excessive vibration can affect the lifetime of the machine and, for example, in paper machines, it can directly affect production quality. Hence, it is important to monitor vibrations. Typically the vibrations are measured with piezo-based accelerometers attached to the bearing housing. Installation of the accelerometers and especially cabling is laborious and expensive in the case of existing machines that have several components to monitor. In continuous process maintenance, a break may be required as well. Therefore, typically only the critical rotors will be monitored, if at all. This research focuses on applying wireless microelectromechanical systems (MEMS) accelerometers to the measurement of large rotor vibration. The results indicated that MEMS accelerometers combined with wireless communication can offer a viable alternative to more expensive piezo-based accelerometers with traditional wire-based communication. The combination provides a flexible and cost-effective method for the collection of vibration data from large rotors and rotor systems.

INDEX TERMS Internet of Things (IoT), microelectromechanical systems (MEMS), accelerometer, subcritical vibration, large rotor, wireless condition monitoring.

I. INTRODUCTION

Large rotating machines are widely used, such as at factories, ships and power plants. Each rotating machine vibrates. If the vibrations are excessive, they can pose problems to the usage of the machine and reduce its lifetime. To measure the vibrations and monitor the machine behavior, integrated electronics piezo-electric (IEPE) accelerometers are typically adopted. However, they need to be physically connected to the measurement module by cabling, which can make the setup of the sensors with existing machines expensive, especially if the machine has several rotating components. A paper machine is an example of a machine which can have more than a hundred rotating rolls. Due to the high cost, only the critical rotating components are typically equipped with sensors.

Large rotors in industrial sized rotating machines can weigh several hundred or thousand kilograms. The rotors are typically operated below the critical speed of the rotor [1]. In those cases, vibrations are subcritical harmonic vibrations, which occur when the rotor is rotating at a fraction of the critical speed. If the rotational frequency of the rotor is, for instance, one half, one third or one fourth of the critical speed, vibration can occur. These are called harmonic components. Fig. 1 presents a schematic figure of subcritical vibrations. Although the speed of the rotor remains below the critical speed, the vibration appears at the natural frequency because the rotor can have several excitations per revolution. If the rotor is rotating at one third of the critical speed and is subjected to three excitations per revolution, the vibration occurs at the natural frequency and a resonance is observed.

Microelectromechanical systems (MEMS) technology has been advanced by the growing demand for cellular phones and tablets. This technology enables cost-effective accelerometer production. Prices are decreasing while accuracy is improving, which has provided new applications for MEMS accelerometers. The typical maximum sampling rate of a MEMS accelerometer is a few kilohertz and large rotors are typically operated below critical speeds. Hence, the operating frequencies are low enough for the

The associate editor coordinating the review of this manuscript and approving it for publication was Macarena Espinilla.

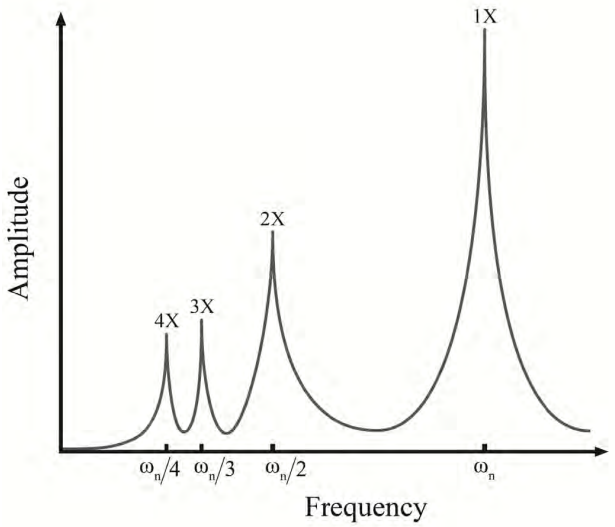

FIGURE 1. Schematic figure of the subcritical vibrations. ω_n is natural frequency of the system and 1X, 2X, 3X and 4X are harmonic components.

MEMS accelerometers to measure rotor vibrations. In addition, MEMS sensors are compact and they have low power consumption. These features are useful in the internet of things (IoT) applications because typically a small size and battery powered operation are required of IoT sensors. Piezo-based accelerometers are widely adopted in industry but new MEMS accelerometers can replace them in some applications. The MEMS accelerometers have been investigated for condition monitoring and compared to IEPE accelerometers [2]–[9].

Albarbar *et al.* [6], [9] tested the performance of MEMS accelerometers and compared the results with an IEPE accelerometer with a particular interest in sinusoidal, random and impulse excitations. They compared one capacitive MEMS accelerometer with an IEPE accelerometer and observed that the MEMS accelerometer performed well with different excitations [9]. However, some phase shift was observed when the MEMS accelerometer was exposed to sinusoidal or random excitations. They conducted similar tests using three different capacitive MEMS accelerometers [6]. In addition, they tested them in a CNC machine to see how they operated in real industrial conditions. In laboratory tests, two of the three MEMS accelerometers received results similar to those observed in [9]. However, the performance of one of the MEMS accelerometers was poor for unknown reasons. The two well-performing accelerometers proved that MEMS accelerometers could be feasible for machine condition monitoring. The fundamental speed and line frequencies were captured as well as their multiplies.

The communication between a microcontroller and MEMS accelerometer and the way the data are saved or transmitted have significant effects on the sampling rate. Chan and Huang [3] investigated the performance of a MEMS accelerometer and a microcontroller. They applied a universal asynchronous receiver transmitter (UART) to transfer the data from the microcontroller to a computer in real-time. The bandwidth of the UART was the limiting factor for the data rate. However, when they used a batch transfer method, they observed a sampling time limitation as the microcontroller could only save a limited amount of data to the static random access memory (SRAM). In addition, when they tested jitter in their system, they reported that it can cause sidebands in the measurement data [3]. For this reason, it is important to stabilize the triggering of the measurement.

To investigate different methods for vibration measurement, accelerometers have been mounted to the surface of the rotor. Elnady *et al.* [7], [8] explored this method with wireless MEMS accelerometers to see whether it would be possible to identify the critical speed of a rotor [7]. They were able to measure the critical speed of the rotor, which, however, did not show as a frequency peak in the plot. The critical speed was detected as a mean value of two peaks present in the frequency plot. These peaks occurred when the velocity was close to a harmonic component. In addition, they compared a finite element model and an analytical model of an on-shaft accelerometer and employed the measurement to validate the models [8].

Feng *et al.* [4] investigated the condition monitoring of a reciprocating compressor by attaching a MEMS accelerometer on the shaft of the flywheel. They examined different leakage fault cases and found that when monitoring the pressure together with the fundamental speed and the third harmonic components of the vibration of the rotor, it is possible to detect faults in the compressor.

In the previous studies, the MEMS accelerometer was placed on the surface of the rotor [4], [7], [8] but Jiménez *et al.* [2] inserted the MEMS accelerometer inside the rotor. They compared three different imbalance conditions and used eddy current sensors to verify the accelerometer results [2]. They measured vibrations during an impulse where they observed the same phenomenon as Elnady *et al.* [7], i.e., the data from the accelerometer showed frequency peaks at both sides of the resonance frequency.

MEMS accelerometers have also been analyzed when monitoring the condition of a wind turbine blade [5]. Typically, the blade condition has been monitored with piezoelectric accelerometers, but they are bulkier and more expensive than the MEMS accelerometers. The small size of the MEMS accelerometers allows for the fixing of the sensor on the blade during manufacturing or retrofitting it afterwards. These studies have stated that it is possible to utilize MEMS accelerometers for monitoring the condition of a wind turbine blade.

In recent years, 3G, 4G and wireless local area networks (WLAN) have become a part of everyday life, allowing easy access to the internet. Wireless sensor networks (WSN) have been tested by exploiting wireless communication technologies [10], [11]. MEMS sensors are typically applied in these studies because of their low energy consumption and low price. Typically, at least one sensor is connected to an outside network, which allows it to connect to the internet and send

information to a server, where the data are stored and are easily accessible. However, as WSN facilitates data collection, the amount of data can increase rapidly, which can challenge the data storing and transmission [10], [12].

In rotating machinery, the sensor sampling rate may need to be relatively high in some situations in order to measure the vibration accurately. When measuring the bearing vibration of an AC motor, the frequencies of interest typically rise between 1-5 kHz [13]. The sampling rate needs to be at least twice the highest frequency of interest, as the Nyquist-Shannon sampling theorem presents [14]. If the system has several rotating components, the amount of data can be large. As a way of minimizing the volume of data transferred and the transfer time, data compressing has drawn research interest [15]–[18]. Compressing the data also lowers the power consumption [16]. However, information can be lost from the original data when compressed [17].

A paper machine is a representative example of an item of rotating machinery that has several rotating rolls which requires vibration measurements ensure the high quality of production. However, attaching sensors to existing machine lines is a costly process. The cabling is time consuming and the setup process may require an expensive maintenance break. Therefore, a wireless sensor unit was built and tested. The sensor unit could be mounted to the machine without a maintenance break. MEMS accelerometers are more economical, consume less energy and are more compact compared to IEPE accelerometers. The MEMS sensors can be installed to each rotor of the machine and not merely for the critical rotors.

This benefits a digital twin as well, which collects data from the physical entity and the data can be exploited to optimize the operation of the product or machine [19]. In addition, the data can be utilized in product development to make the product more optimally suit the designed application.

II. METHODS

A. SENSOR UNIT

A sensor unit was built to investigate whether a MEMS accelerometer can be used to measure large rotor vibrations. The sensor unit adopted wireless communication to transfer the data.

1) COMPONENTS AND STRUCTURES

The sensor unit included the following components:

- Pycom's WiPy 3.0 (IoT development platform)
- Pycom's Expansion board 2.0 (expansion board for the WiPy 3.0)
- ADXL355 (MEMS accelerometer)
- battery (2500 mAh, 3.7 V)

The WiPy 3.0 (Pycom) development platform had an ESP32 microcontroller chip, which contains a built-in radio module for WLAN. It had two cores: one core typically operated the WLAN radio and wireless communication and the other executed other tasks. Two cores helped to optimize the performance of the controller. Table 1 presents the specifications of ESP32.

TABLE 1. Specification of ESP32 microcontroller Chip.

Specifications	ESP32
Microcontroller Unit	Tensilica Xtensa 32-bit LX6
Cores	2
Clock frequency (MHz)	240
SRAM (KiB)	520
802.11 b/g/n WI-FI	HT40
GPIO	36
SPI/I2C interfaces	4/2

TABLE 2. Specifications of ADXL355 and HS-1005005001.

	ADXL355	HS-1005005001
Measurement range (g*)	(±2, ±4, ±8)	±16g*
Sensitivity (µg*/digit)	(3.9, 7.8, 15.6)**	500 (mV/g*)
Sample rate (Hz)	3.906 – 4000	2 – 10000
Noise density (µg*/Hz)	25	-
Number of axis	3	1

*g = gravitational acceleration
**Depends on the measurement range

WiPy 3.0 was connected to Expansion board 2.0 (Pycom), which enabled the powering of the controller with a battery. The microcontroller was programmed with Arduino IDE and C/C++ language.

The MEMS accelerometer was a capacitive accelerometer ADXL355 (Analog devices). The results from the ADXL355 accelerometer were compared to data from a Hansford sensors' HS-1005005001 IEPE accelerometer (Fig. 2 b). Table 2 presents the specifications of both accelerometers.

The cDAQ-9191 wireless data acquisition unit and NI-9234 sound and vibration input module by National Instruments were used to acquire the data from the reference accelerometer (HS-1005005001) (Fig. 2). The cDAQ-9191 wireless data acquisition unit allowed wireless communication between the apparatus and the computer. However, cabling was still required to attach the sensors to the NI-9234 module.

The casing of the built sensor unit (Fig. 3) was manufactured from aluminum with a CNC milling machine. ADXL355 and Expansion board 2.0 was screwed to the casing, double-sided tape kept the battery in place, and magnets with threads kept the sensor unit in place during the measurement.

2) OPERATION PRINCIBLE

The sensor unit was controlled with a browser-based graphical user interface (GUI). Fig. 4 presents the operating principle and the procedure is explained below.

1. The server sent a UDP packet to the sensor unit when the user started the measurement from the GUI. The

FIGURE 2. (a) National Instruments' cDAQ-9191 wireless data acquisition unit and NI-9234 sound and vibration input module. (b) Hansford sensors' HS-1005005001 IEPE accelerometer. HS-1005005001 has a magnet attached to the bottom of the sensor.

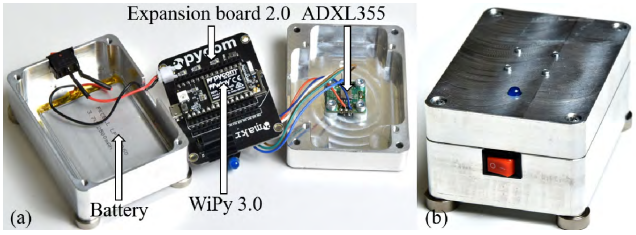

FIGURE 3. Built sensor unit. (a) presents components of sensor unit and (b) presents the assembled sensor unit.

packet contained information about the sampling rate, sampling time and which axes were used.
2. The sensor unit started the measurement according to the information received from the server.
3. WiPy 3.0 read the measurement data from the sensor and saved it to the RAM of the microcontroller.
4. When 48 samples were saved to the RAM, the sensor unit sent the data on the server using UDP.
5. Steps 3 and 4 were repeated until the sampling time finished.
6. The sensor unit sent a UDP packet to the server to indicate that the measurement was finished.
7. Server saved the data to an ASCII-file.

3) POWER CONSUMPTION

Power consumption can be separated into two states: measurement state (explained in Fig. 4) and idle state. In the idle state, the sensor unit is waiting for messages from the server while all other functions are turned off. In the measurement state, the average power consumption from the battery is 490 mW (current consumption is 132 mA) and in the idle state it is 160 mW (current consumption is 42 mA).

B. SIGNAL PROCESSING

The ADXL355 accelerometer outputs the acceleration as a digital value, which is formatted as a 20-bit two's complement value. The data were converted to m/s^2 using the scale factor of 3.9 μg/LSB and gravitational acceleration.

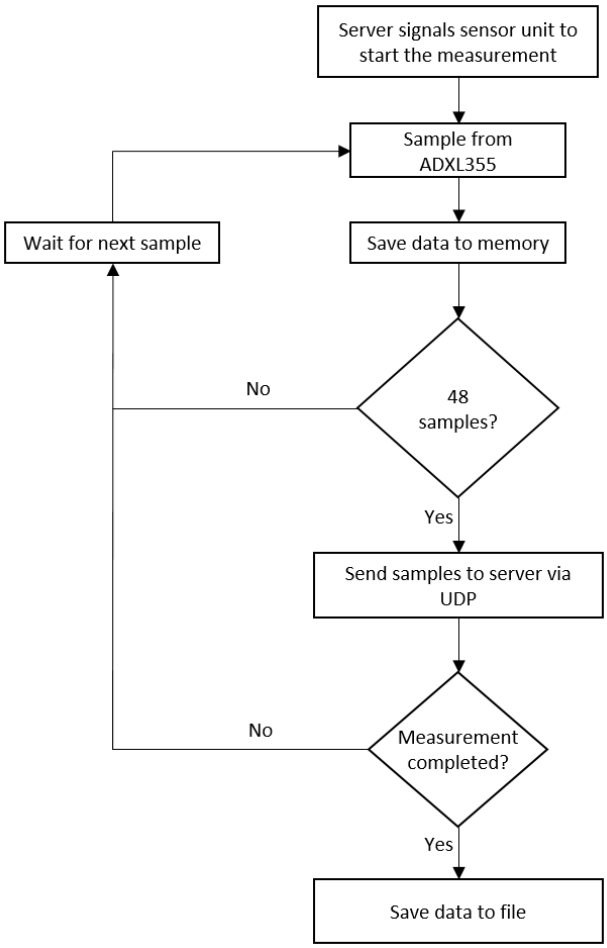

FIGURE 4. The operating principle of sensor unit.

1) LOW-PASS FILTER

ADXL355 has its own built-in low-pass filter set to 1/4 of the sampling rate. The accelerometer also has a built-in high-pass filter as well, but it was deactivated. The test rotor was sampled at 1000 Hz, indicating that the cut-off frequency of the low-pass filter was 250 Hz. The first bending mode natural frequencies (around 25 Hz in x direction and 29 Hz in y direction) of the rotor denote that frequencies below 50 Hz are the interesting frequencies when investigating the subcritical vibration behavior of a large rotor.

2) FOURIER ANALYSIS

Fourier transform converts a time domain signal into the frequency domain. The principle of the Fourier transform is that any signal can be divided into an infinite amount of sinusoidal functions, which reveals the frequencies and amplitudes of the signal components [20]. In rotating machinery, vibrations are typically monitored to prevent damage on the machine or a reduction on the production quality. The vibration frequency and amplitude are the interesting components of the data. Hence, Fourier transform is applied. However, Fourier analysis may need ample computing power as the amount of data increases. To expedite the transform

FIGURE 5. Paper machine roll used during this study in the CNC grinding machine.

calculations, Cooley and Tukey [21] developed a faster method to perform numerical Fourier transfer called the fast Fourier transform (FFT). FFT applies complex numbers to reduce the required computing power.

For the measured acceleration data, FFT was applied in the form of a short-time Fourier transform (STFT). STFT makes possible the observation of frequency change over time [22]. It divides the original time domain signal into smaller segments and takes the FFT measurement from each segment separately. The method allows the monitoring of the frequencies in one selected time window and represents all of the segments as a 3D plot, which has time (s), frequency (Hz) and amplitude (m/s^2) as axes. These plots are called spectrograms. Spectrograms are widely exploited in sound and speech analysis [23]–[25] but can also be applied to the analysis of how vibrations change over time.

When the vibrations are measured during a rotor acceleration, the measured signal is not periodic. Hence, the signal is manipulated to mimic a periodic signal using windowing function, thus making FFT feasible. In the present study, Hanning window was applied.

C. ROTOR SETUP

The measurements were made with a paper machine roll (Fig. 5). The roll was mounted to a CNC grinding machine, which controlled the acceleration and speed of the roll. The right side of the roll was the driving side and the left side was the tending side. Fig. 6 presents the dimensions of the paper machine roll. The roll weighed approximately 720 kg.

The sensor units and reference accelerometers were fixed to the bearing housings with magnets (Fig. 7). The reference accelerometers were located on the top and side of the bearing housing, since one sensor can only measure one direction. The sensor unit can measure accelerations in three directions, thus one sensor unit per bearing housing sufficed. Both bearing housings were equipped with sensors.

D. MEASUREMENT PROCEDURE

The measurement was made during an acceleration from 0 to 1060 rpm with an approximate acceleration of 0.62 rad/s^2 (5.9 rpm/s^2). The sampling rate of the sensor unit was set to 1000 Hz. STFT was exploited to observe the results from the measurement.

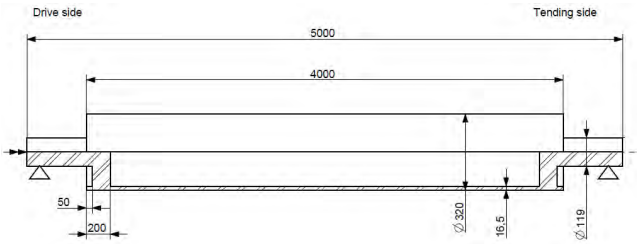

FIGURE 6. Dimensions of the paper machine roll.

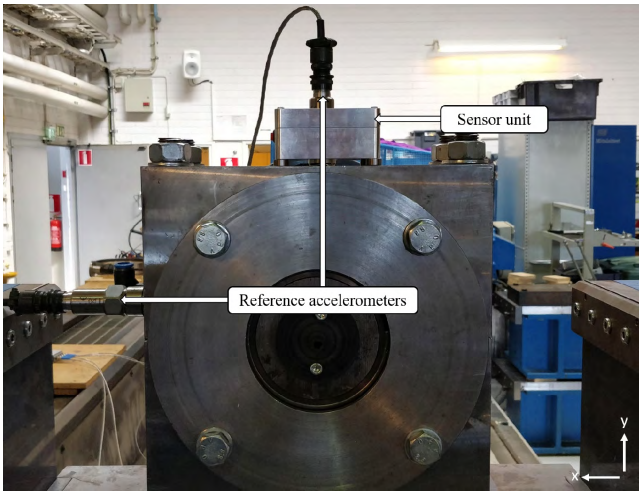

FIGURE 7. The measurement setup of the tending side. Two reference accelerometers and one sensor unit were installed for both bearing housings.

The sweep measurement proceeded as follows:

1. One sensor unit and two reference sensors were mounted to both the drive and the tending side bearing housings (Fig. 7).
2. The rotor was accelerated from 0 to 1060 rpm while measuring the acceleration of the bearing housing

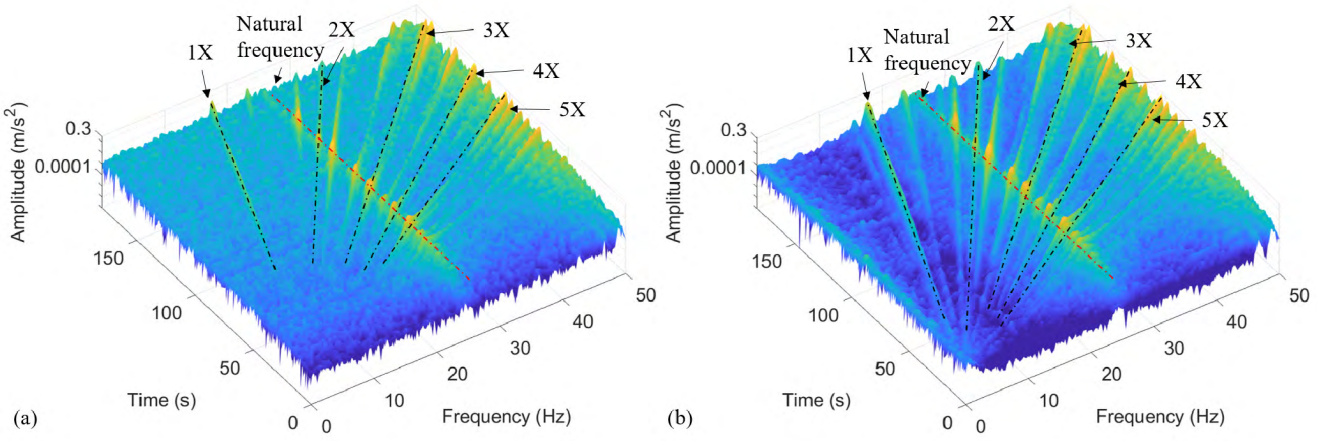

FIGURE 8. Horizontal vibration of the tending side of the roll. 1X, 2X, 3X, 4X and 5X represent harmonic components of vibration. Natural frequencies marked in the picture are the natural frequency of the first bending mode. (a) presents data from the MEMS accelerometer and (b) presents data from the reference accelerometer.

in x (horizontal) and y (vertical) directions. The sensor units had a sampling rate of 1000 Hz and the reference accelerometers had an approximate sampling rate of 1650 Hz.

3. Data processing and plots were realized with MATLAB.

To compare the amplitudes of the vibration received from the sweep acceleration measurements, a step-by-step sweep measurement was made. However, only the reference accelerometers were applied during this measurement. The measurement was conducted by accelerating the rotor from 240 to 1060 rpm in 6 rpm steps. After each step, a measurement was taken when the rotor was rotating at a constant speed.

The step-by-step sweep measurement proceeded as follows:

1. Reference accelerometers were mounted to the bearing housing as presented in Fig. 7. The approximate sampling rate of the sensors was 1650 Hz.
2. The rotor was accelerated to 240 rpm before the measurement was started.
3. The first measurement was taken at that speed. The measurement lasted 5.45 seconds.
4. The rotor was accelerated by 6 rpm and a new measurement was taken when the speed was stabilized.
5. Step 4 was repeated until the speed of 1060 rpm was achieved. Every measurement lasted approximately 5.45 seconds.
6. Data processing and plots were realized with MATLAB.

III. RESULTS

Figures from 8 to 11 present the vibrations during the sweep measurement, as the rotor was constantly accelerated. 1X, 2X, 3X, 4x and 5X point to the harmonic components of the vibrations. 1X presents the first harmonic component, which is equal to the rotational velocity of the rotor, 2X presents the second harmonic component, 3X presents the third harmonic component etc. The natural frequency marked in the picture presents the natural frequency of the first bending mode.

Fig. 8 and Fig. 9 present vibrations at the tending side of the rotor and Fig. 10 and Fig. 11 present the vibrations on the driving side of the rotor. The vibrations occurring in the vertical direction (Fig. 9 and Fig. 11) have lower amplitudes compared to horizontal direction (Fig. 8 and Fig. 10). The MEMS and reference sensors measured a horizontal natural frequency between 25 Hz and 25.3 Hz and the vertical natural frequency between 29.3 Hz and 29.5 Hz according to the MEMS sensors, and between 29.3 Hz and 29.7 Hz according to the reference accelerometers.

The frequency peaks received from the step-by-step sweep measurement were compared to the peaks received from the step-by-step sweep measurements. Table 3 and Table 4 present the amplitudes and frequencies of the frequency peaks measured from the driving and of the rotor with the MEMS and reference accelerometers during the step-by-step sweep measurement, and reference accelerometers during sweep measurement. Fig. 12 presents the spectrogram of the step-by-step sweep measurement and sweep measurement side by side.

IV. DISCUSSION

The sensor unit was able to measure the required vibrations. The main harmonic components (the first, second, third, fourth and fifth harmonic components) and the natural frequency of the first bending mode could be observed from the data. There were other non-integer harmonic components present in the spectrograms as well, which were produced by the bearings. The outer ring of the bearing is the cause of most of these vibrations. The equations are presented e.g., by [26]. Fig. 13 identifies some of the vibration components caused by the outer rings of the bearings.

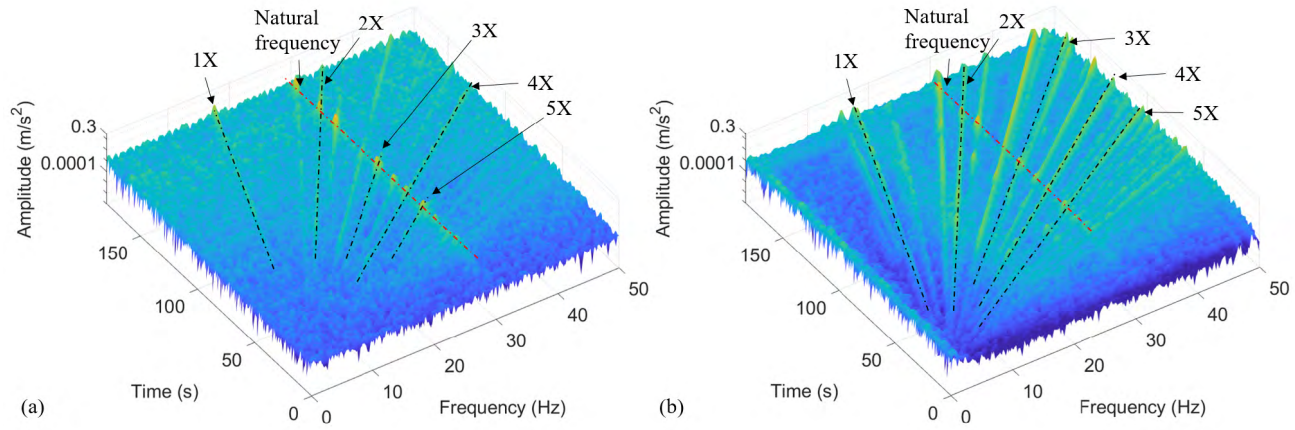

FIGURE 9. Vertical vibration of the tending side of the roll. 1X, 2X, 3X, 4X and 5X represent harmonic components of vibration. Natural frequencies marked in the picture are the natural frequency of the first bending mode. (a) presents data from the MEMS accelerometer and (b) presents data from the reference accelerometer.

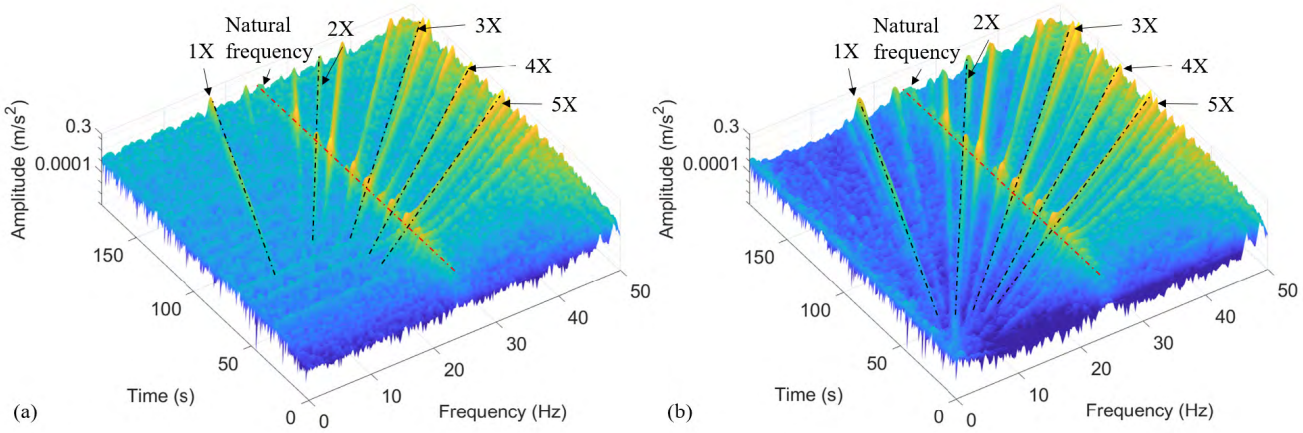

FIGURE 10. Horizontal vibration of the driving side of the roll. 1X, 2X, 3X, 4X and 5X represent harmonic components of vibration. Natural frequencies marked in the picture are the natural frequency of the first bending mode. (a) presents data from the MEMS accelerometer and (b) presents data from the reference accelerometer.

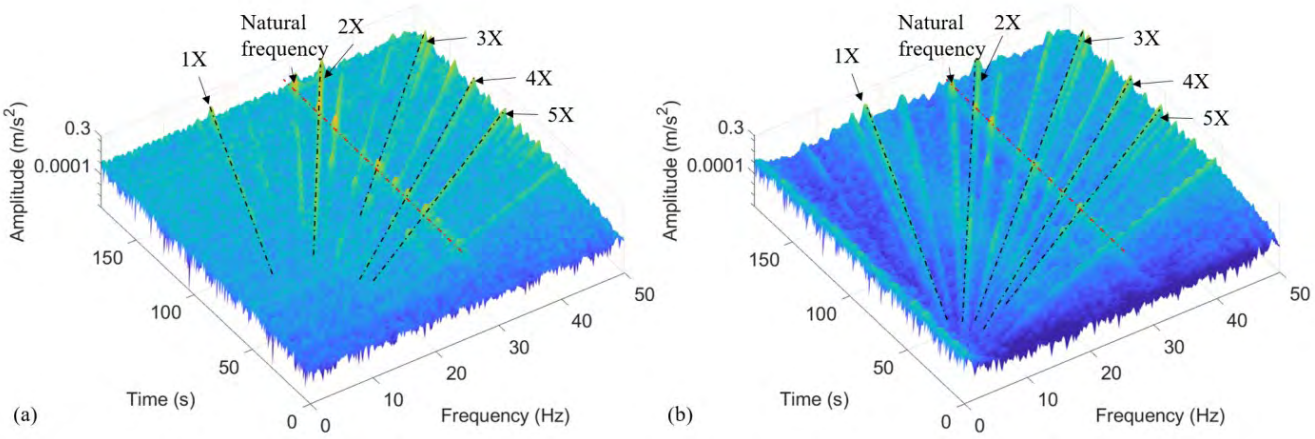

FIGURE 11. Vertical vibration of the driving side of the roll. 1X, 2X, 3X, 4X and 5X represent harmonic components of vibration. Natural frequencies marked in the picture are the natural frequency of the first bending mode. (a) presents data from the MEMS accelerometer and (b) presents data from the reference accelerometer.

Natural frequencies were presented clearly in the sensor unit data and they were similar to the natural frequencies captured with reference sensors. However, as observed in Table 3 and 4, the amplitudes of the frequency peaks

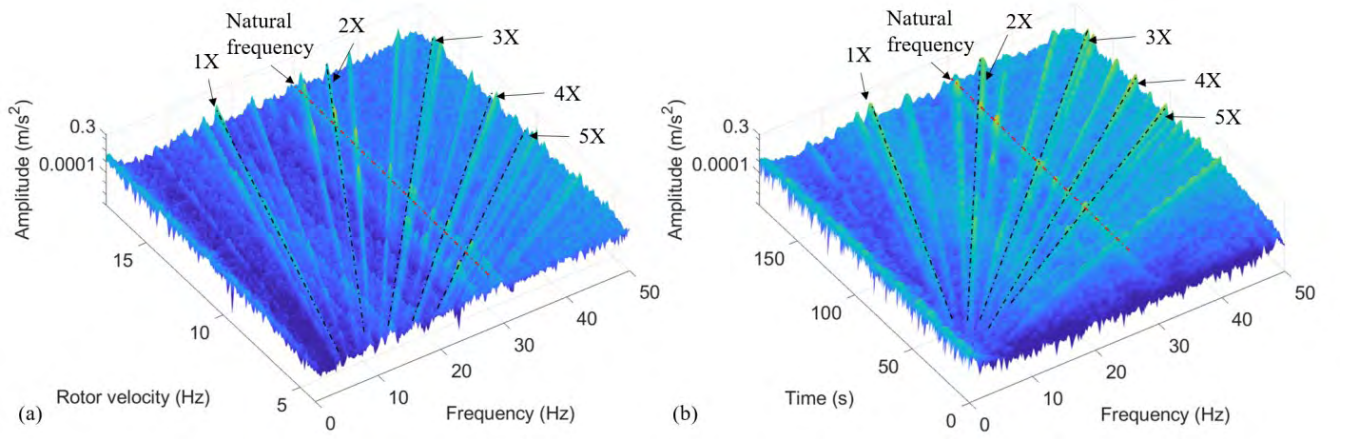

FIGURE 12. Vertical vibration of the driving side of the roll. 1X, 2X, 3X, 4X and 5X represent harmonic components of vibration. Natural frequencies marked in the picture are the natural frequency of the first bending mode. (a) presents data from step-by-step sweep measurement with the reference sensor and (b) presents data from sweep measurement with the reference sensor.

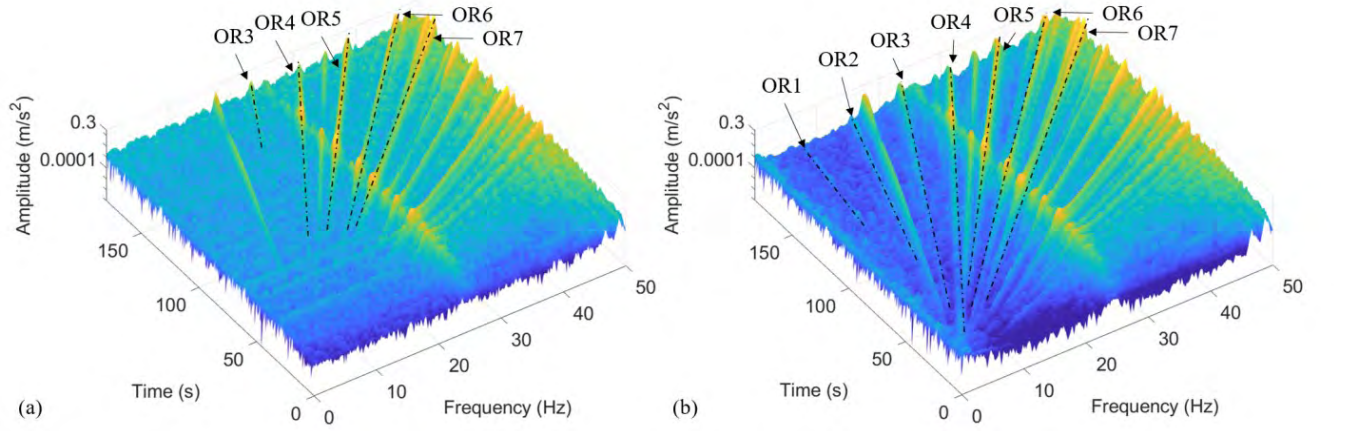

FIGURE 13. Vibrations caused by the outer bearing ring in horizontal direction of the driving side. The seven first harmonic components of the outer bearing ring are marked with OR1 to OR7. (a) presents data from the MEMS accelerometer and (b) presents data from the reference accelerometer.

TABLE 3. Natural frequencies (f) and their amplitudes (A) on the driving side of the rotor in vertical direction.

Harmonic subcritical resonances	MEMS sensor		Reference sensor (sweep measurement)		Reference sensor (step-by-step sweep measurement)	
	A (m/s^2)	f (Hz)	A (m/s^2)	f (Hz)	A (m/s^2)	f (Hz)
2	0.027	29.5	0.023	29.7	0.044	29.4
3	0.016	29.3	0.013	29.3	0.016	29.4
4	0.010	29.5	0.010	29.7	0.014	29.6
5	0.012	29.5	0.016	29.3	0.020	29.6

TABLE 4. Natural frequencies (f) and their amplitudes (A) on the driving side of the rotor in horizontal direction.

Harmonic subcritical resonances	MEMS sensor		Reference sensor (sweep measurement)		Reference sensor (step-by-step sweep measurement)	
	A (m/s^2)	f (Hz)	A (m/s^2)	f (Hz)	A (m/s^2)	f (Hz)
2	0.055	25.0	0.052	25.0	0.050	25.3
3	0.087	25.0	0.072	25.0	0.076	25.5
4	0.078	25.3	0.067	25.0	0.056	25.5
5	0.11	25.0	0.12	25.0	0.21	25.5

were not similar when the measurement was taken during the rotor constant acceleration (sweep measurement) and during step-by-step acceleration. The signal is not periodic and the vibrations are changing constantly during the measurement. Hence, the amplitudes depend on how long segments are taken from the data when the spectrograms are made. If the segment is long, there are less peaks at a certain frequency compared to the length of the segment, which indicates lower amplitudes for the peaks. In contrast, if the segment is short, there are more peaks compared to the length of the segment, which indicates that the amplitudes are higher.

There was a difference between the magnitudes of the vertical and horizontal frequency peaks due to the foundation stiffness of the rotor system. The foundation was more

rigid in the vertical than in horizontal direction, and thus the amplitudes of the vertical vibrations were lower and the first bending mode natural frequency was higher.

The results show that the MEMS accelerometers were suitable for measuring the subcritical vibrations of a large rotor from the bearing housing. This will open new opportunities to collect more data from the large rotating machineries. The installation needs minimal effort and the sensors are cost effective, which makes possible the measurement of several components of the machine instead of merely the critical components. More data can be measured, and the usage of the machine can be better optimized. Furthermore, the need for maintenance can be estimated more accurately.

The digital twin of a rotor can also benefit from the sensor units. They can be connected to the internet, which makes it possible to send the data easily to a digital twin. These sensors are controlled over WLAN and by opening the network to the internet, they could be controlled from a distance. This is beneficial for digital twins. In addition, with the sensor units, digital twin can receive more data from the physical machine because more components of the machine can be monitored.

This paper suggests that the MEMS accelerometers are suitable for monitoring the vibration of a large rotor. However, wireless communication still needs more research in order to establish more reliable data transfer. The data were sent during the measurement, which connoted that there was a limited time window in which the data could be transferred. To establish sufficiently fast communication, the user diagram protocol (UDP) was utilized. However, its downside was that it did not check if the data reached its destination. Occasionally some of the data were subsequently lost during the transfer. This could be prevented by saving the data to a memory during the measurement and by sending it forward when the measurement is finished. This way, a slower but more reliable communication protocol could be adopted, since it will not interfere with the measurement process.

Another interesting approach to the vibration measurement of a large rotor could be to attach the sensor unit to the rotor. In this way the sensor would rotate with the rotor and reveal more information about the rotor behavior. These types of studies have been conducted for smaller-scale rotors [2], [4], [7], [8] but not for large-scale ones.

V. CONCLUSION

The present study investigated a more cost-effective and easier way to measure vibrations from large rotating machines. It is time consuming and expensive to mount a wired sensor to already existing machines that include several rotating components. This problem was addressed with a wireless sensor unit, which contained a MEMS accelerometer and a microcontroller with a WLAN module to transfer data. The sensor unit was powered by battery without a need for cabling, which allowed implementation with minimal effort. The measurement was made from a bearing housing and one sensor unit could measure acceleration in three directions. Therefore, only one unit was required per bearing housing.

The results verified that the sensor unit could measure vibrations from large rotors. The harmonic components and natural frequencies of the rotor could be observed from the results. In addition, bearing vibrations could also be detected. The amplitudes of the harmonic vibration components varied from the real amplitudes (i.e., amplitudes measured with constant speed at that rotation speed) because the measurement was taken during a constant acceleration of a rotor and the vibration was constantly changing. In such as case the signal is not periodic. Hence the incorrect amplitudes were not induced by a sensor unit defect, but they were inflicted by the measurement procedure.

ACKNOWLEDGMENT

The authors would like to thank Mr. Ville Klar for his contribution to the development of the sensor unit.

REFERENCES

[1] R. Viitala, T. Widmaier, and P. Kuosmanen, "Subcritical vibrations of a large flexible rotor efficiently reduced by modifying the bearing inner ring roundness profile," *Mech. Syst. Signal Process.*, vol. 110, pp. 42–58, Sep. 2018.

[2] S. Jiménez, M. O. T. Cole, and P. S. Keogh, "Vibration sensing in smart machine rotors using internal MEMS accelerometers," *J. Sound Vib.*, vol. 377, pp. 58–75, Sep. 2016.

[3] Y. J. Chan and J.-W. Huang, "Multiple-point vibration testing with microelectromechanical accelerometers and micro-controller unit," *Mechatronics*, vol. 44, pp. 84–93, Jun. 2017.

[4] G. Feng, N. Hu, Z. Mones, F. Gu, and A. D. Ball, "An investigation of the orthogonal outputs from an on-rotor MEMS accelerometer for reciprocating compressor condition monitoring," *Mech. Syst. Signal Process.*, vols. 76–77, pp. 228–241, Aug. 2016.

[5] O. O. Esu, J. A. Flint, and S. J. Watson, "Condition monitoring of wind turbine blades using MEMS accelerometers," *Renew. Energy World Eur.*, pp. 1–12, Jun. 2013.

[6] A. Albarbar, S. Mekid, A. Starr, and R. Pietruszkiewicz, "Suitability of MEMS accelerometers for condition monitoring: An experimental study," *Sensors*, vol. 8, no. 2, pp. 784–799, 2008.

[7] M. E. Elnady, J. K. Sinha, and S. O. Oyadiji, "Identification of critical speeds of rotating machines using on-shaft wireless vibration measurement," *J. Phys., Conf. Ser.*, vol. 364, no. 1, 2012, Art. no. 012142.

[8] M. E. Elnady, A. Abdelbary, J. K. Sinha, and S. O. Oyadiji, "FE and experimental modeling of on-shaft vibration measurement," in *Proc. 15th Int. Conf. Aerosp. Sci. Aviation Technol.*, May 2013, pp. 1–18.

[9] A. Albarbar, A. Badri, J. K. Sinha, and A. Starr, "Performance evaluation of MEMS accelerometers," *Measurement*, vol. 42, no. 5, pp. 790–795, 2009.

[10] S. Lu, P. Zhou, X. Wang, Y. Liu, F. Liu, and J. Zhao, "Condition monitoring and fault diagnosis of motor bearings using undersampled vibration signals from a wireless sensor network," *J. Sound Vib.*, vol. 414, pp. 81–96, Feb. 2018.

[11] R. S. Carbajo, E. S. Carbajo, B. Basu, and C. M. Goldrick, "Routing in wireless sensor networks for wind turbine monitoring," *Pervas. Mobile Comput.*, vol. 39, no. 2, pp. 1–35, Aug. 2017.

[12] M. Xia, T. Li, Y. Zhang, and C. W. de Silva, "Closed-loop design evolution of engineering system using condition monitoring through Internet of things and cloud computing," *Comput. Netw.*, vol. 101, pp. 5–18, Jun. 2016.

[13] A. Vogl, D. T. Wang, P. Storås, T. Bakke, M. M. V. Taklo, A. Thomson, and L. Balgård, "Design, process and characterisation of a high-performance vibration sensor for wireless condition monitoring," *Sens. Actuators A, Phys.*, vol. 153, no. 2, pp. 155–161, 2009.

[14] H. Nyquist, "Certain topics in telegraph transmission theory," *Proc. IEEE*, vol. 90, no. 2, pp. 280–305, Feb. 2002.

[15] W. Guo and P. W. Tse, "A novel signal compression method based on optimal ensemble empirical mode decomposition for bearing vibration signals," *J. Sound Vib.*, vol. 332, no. 2, pp. 423–441, 2013.

[16] Q. Huang, B. Tang, L. Deng, and J. Wang, "A divide-and-compress lossless compression scheme for bearing vibration signals in wireless sensor networks," *Measurement*, vol. 67, pp. 51–60, May 2015.
[17] W. Bao, W. Wang, R. Zhou, N. Li, J. Yang, and D. Yu, "Application of a two-dimensional lifting wavelet transform to rotating mechanical vibration data compression," *Proc. Inst. Mech. Eng., C, J. Mech. Eng. Sci.*, vol. 223, no. 10, pp. 2443–2449, 2009.
[18] M. Oltean, J. Picheral, E. Lahalle, H. Hamdan, and J. Griffaton, "Compression methods for mechanical vibration signals: Application to the plane engines," *Mech. Syst. Signal Process.*, vol. 41, nos. 1–2, pp. 313–327, 2013.
[19] S. Haag and R. Anderl, "Digital twin—Proof of concept," *Manuf. Lett.*, vol. 15, pp. 64–66, Jan. 2018.
[20] T. Widmaier, "Optimisation of the roll geometry for production conditions," Ph.D. dissertation, Dept. Eng. Des. Prod., Aalto Univ., Helsinki, Finland, 2012.
[21] J. W. Cooley and J. W. Tukey, "An Algorithm for the machine calculation of complex Fourier series," *Math. Comput.*, vol. 19, no. 90, p. 297, 1965.
[22] E. Sejdić, I. Djurović, and J. Jiang, "Time–frequency feature representation using energy concentration: An overview of recent advances," *Digit. Signal Process., A Rev. J.*, vol. 19, no. 1, pp. 153–183, 2009.
[23] P. K. Ajmera, D. V. Jadhav, and R. S. Holambe, "Text-independent speaker identification using Radon and discrete cosine transforms based features from speech spectrogram," *Pattern Recognit.*, vol. 44, nos. 10–11, pp. 2749–2759, 2011.
[24] B. Pinkowski, "Principal component analysis of speech spectrogram images," *Pattern Recognit.*, vol. 30, no. 5, pp. 777–787, 1997.
[25] B. E. D. Kingsbury, N. Morgan, and S. Greenberg, "Robust speech recognition using the modulation spectrogram," *Speech Commun.*, vol. 25, no. 1, pp. 117–132, 1998.
[26] A. H. Slocum, *Precision Machine Design*. Upper Saddle River, NJ, USA: Prentice-Hall, 1992.

IVAR KOENE was born in 1993. He received the B.Sc. and M.Sc. degrees from Aalto University, in 2016 and 2018, respectively, where he is currently pursuing the Ph.D. degree. During his studies, he was a Research Assistant with a paper machine laboratory. He is focusing on how cost-effective IoT sensors could be utilized in the condition monitoring of large rotating machinery. He is also involved in a digital twin related research, where one of the goals is to utilize digital twin for predictive maintenance.

RAINE VIITALA was born in 1992. He received the M.Sc. and D.Sc. degrees in mechanical engineering from Aalto University, in 2017 and 2018, respectively. In 2018, he visited Technische Universität Darmstadt, researching rotating kinetic energy storages, i.e., flywheels. He has a solid background in experimental large rotor research, including vibration analysis and subcritical vibration, bearing excitations, and roundness measurements and manufacturing for operating conditions. His work can be widely applied in several industrial applications, such as electric motors and generators, turbines, and paper machines. He is involved in developing an AI and simulation enhanced digital twin of a rotor system. He is instructing four doctoral candidates, three master's thesis students, and two bachelor's thesis students. He lectures on a bachelor level course in Mechatronics Basics. He received the Aalto University School of Engineering dissertation award.

PETRI KUOSMANEN was born in 1963. He was appointed as a Full Professor at the Helsinki University of Technology (currently Aalto University), in 1999. He is the Head of Engineering Design, Aalto University. He founded the paper machinery research group, in 1990. He also established the 3D grinding technology of large rotors and innovated optimizing rotors for their operating conditions in industrial environments. He has strongly promoted entrepreneurship in the development of new technology, both in industrial and medical applications.